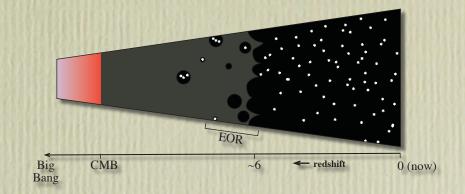# Observing the Epoch of Reionization

Miguel F. Morales

MIT Kavli Institute

January 30, 2007 @ Berkeley

I'm an astrophysics experimentalist, and what I'd like to talk about today is an emerging area of observational cosmology called the EOR, and the US-Australian observatory my colleagues and I are building to measure this new cosmological signature.
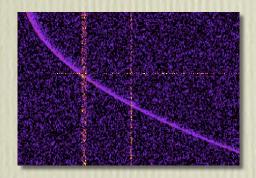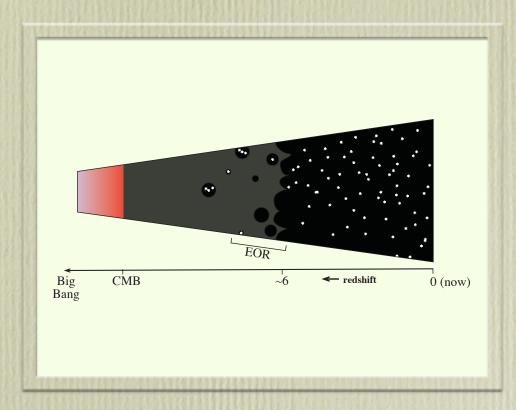
Overview

- ## The EOR Signal

- ## Building an EOR machine: MWA–LFD
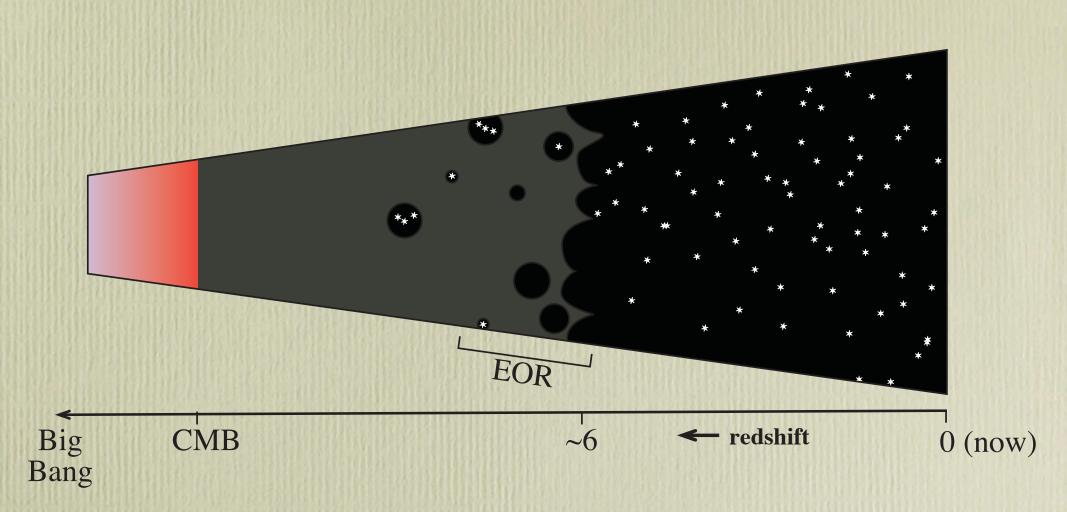

- ## Other radio cosmology signatures...

My talk is divided into 3 sections. First I'll briefly describe what the Epoch of Reionization is and the patterns we are looking for. I'll then spend the majority of the talk describing how to build an EOR observatory, and the instrumentation and techniques we've developed to observe this faint radio emission. Then at the end, if I have time I'll describe some other cosmology signatures I've been developing.

Epoch of reionization signatures

So let me spend a couple of minutes talking about the Epoch of Reionization signal.
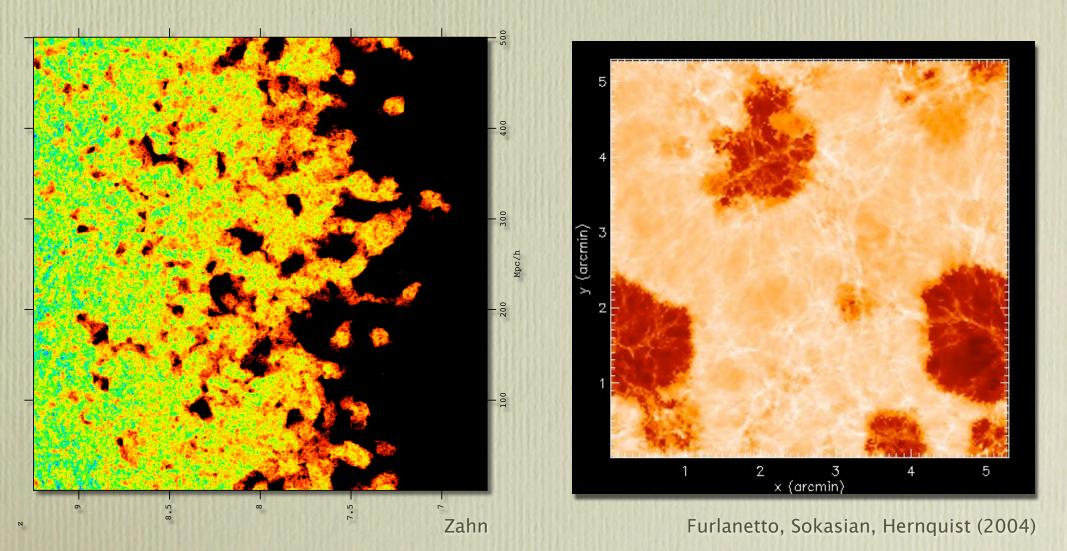
Questions: How does structure form? What are the properties an dynamics of the first luminous objects?

[Short story: CMB 300k years after the big band, neutral, condense into structures 1 billion years, first galaxies and quasars emerge burning off the neutral H, pointing at left hand plot.]

If you are interested in structure formation, this is one of the crucial transitions in the universe as the first galaxies and stars light up and the first heavier elements are forged. Unfortunately it is also extremely difficult to observe. It is very far away and the neutral hydrogen absorbs the light that can be observed with ground based telescopes. However, the neutral HI itself glows at 21 cm through the hyper-fine sin-flip transition, thus we can see the neutral hydrogen glowing at low radio frequencies.

Hɪ during EOR

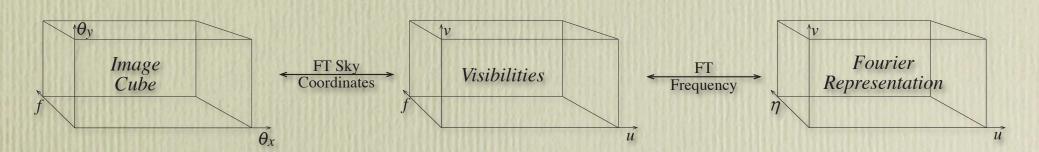Zahn

Furlanetto, Sokasian, Hernquist (2004)

Now let's zoom in on the EOR to see what it might look like. The picture on the left shows a model by Oliver Zahn, as the yellow neutral hydrogen is burned away by the emerging galaxies as a function of redshift. The picture on the right instead shows a slice at one redshift of what one might see. [Filaments of the cosmic web, bubbles.]

This is an incredibly rich data set, in addition to showing how the matter coalesces into the first galaxies and stars, it shows their influence on the surrounding medium. By analyzing the shape and distribution of these bubbles one can determine whether stars or AGN dominated reionization, and whether the first generation of stars hindered or accelerated the formation of the second generation of stars.

Because the signal is very faint, the first generation EOR radio instruments will not be able create images like this. Instead we observe the power spectrum, and study the distribution and sizes of the knots and bubbles using the statistical techniques developed for the CMB.
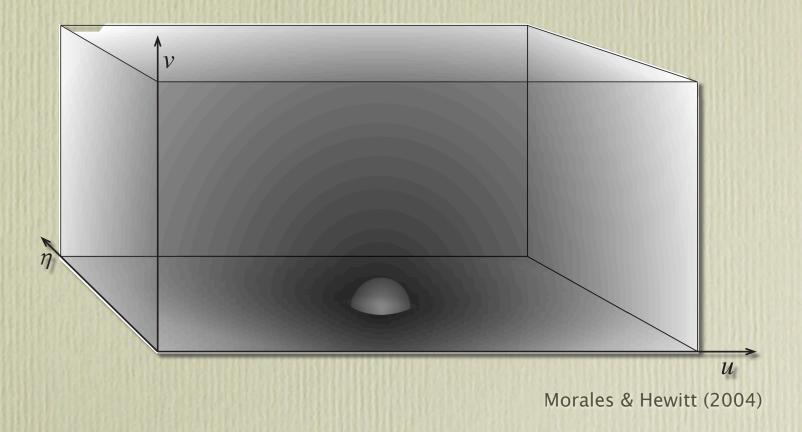
Statistical EOR detection

Morales & Hewitt (2004)

One key difference between the CMB and EOR PS analysis is that the EOR signal is three dimensional. While the CMB is a 2D map from one redshift---a surface, because the 21 cm radiation is an emission line, the observed frequency tells you the redshift and thus the line of sight distance. So instead of a surface you are observing a 3D volume of space, with bright and dark patches related to the density, temperature, and ionization of the neutral hydrogen.

To measure the power spectrum...

This three dimensional nature leads to an important symmetry...
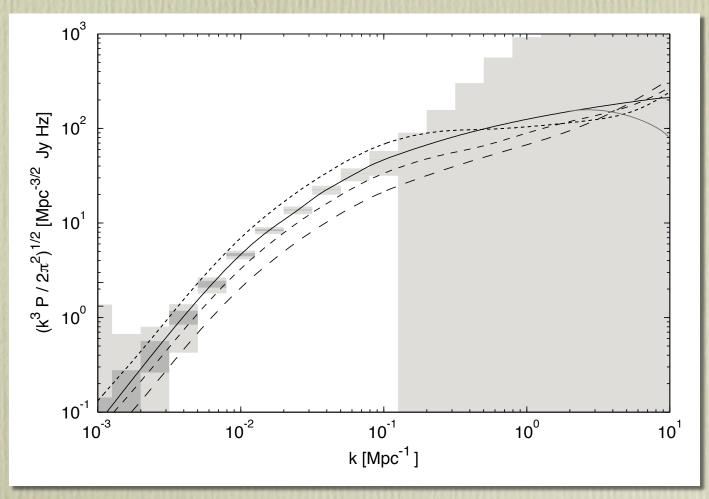
Spherical symmetry

Morales & Hewitt (2004)

Spherically symmetric. Annuli. Useful, almost none of the foregrounds share this symmetry [walk through].

I want you to keep this picture in your head. This three dimensional nature of the signal is very important for understanding the EOR signal: integrating over a whole volume is what gives modern EOR instruments their power, and this symmetry is behind the foreground subtraction techniques which I'll discuss later. And is why our paper introducing this symmetry has been sighted by nearly every subsequent paper on the EOR power spectrum.

If there were no foregrounds....
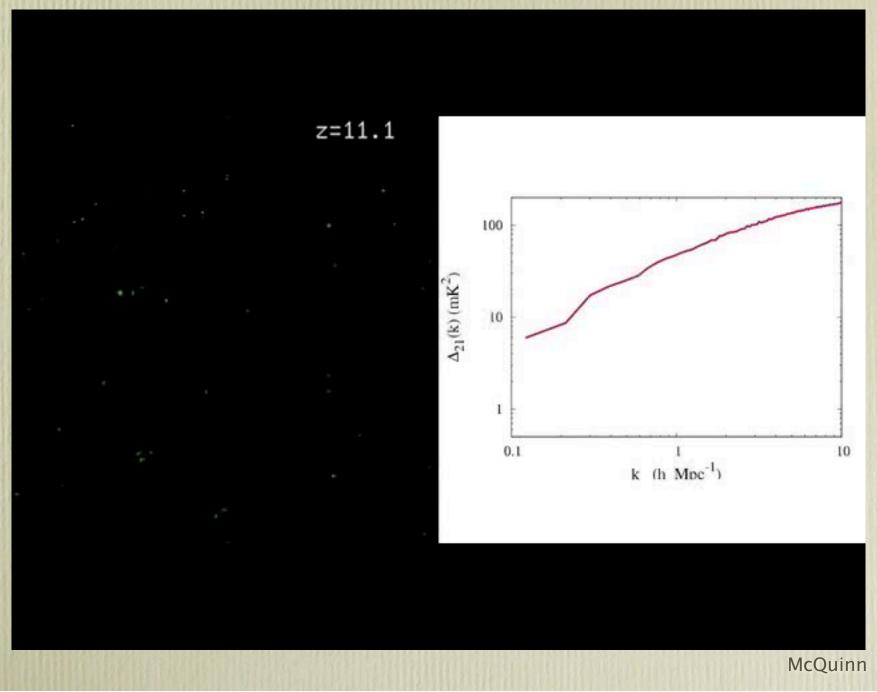
EOR power spectrum

Furlanetto, Zaldarriaga, Hernquist (2004a,b)
Bowman, Morales & Hewitt (2005)
Kaplinghat (2005)

Where this measures the emission in each spherical shell, and the shape of the power spectrum tells us about the sizes and evolution of HI and ionized Stromgren spheres during the EOR.

For example, using a simple model by Furlanetto et al., the signal without any bubbles (fully neutral is here). If bubbles have reionized 25% percent of the universe the line is here. [43%, 51%]. Determining what the shape of the curve may be is a very active area of theoretical work, including all kinds of effects. One fun example introduced by Manoj Kaplinghat is if DM is made of gravitinos, then the NLSP or other WIMP would decay to this particle late. This would mean DM is not thermal and cold, but has a non-thermal component to its velocity from the decay energy, and this non-thermal distribution would erase structure on small scales. This effect is unmeasurable with the CMB, but future EOR observatories may be able to see this kind of signal from gravitino nucleosynthesis.

Power spectrum dynamics

McQuinn

We can actually measure the PS at multiple redshifts, providing a coarse movie of reionization an allowing us to study the dynamics. To give you a feel for this let me play this movie by Matt McQuinn, with the caveat that the simulation box is small and first generation observations are sensitive to larger scales.

By measuring the power spectrum as a function of redshift, we can see the structure form and it's impact on the IGM and subsequent star and galaxy formation.
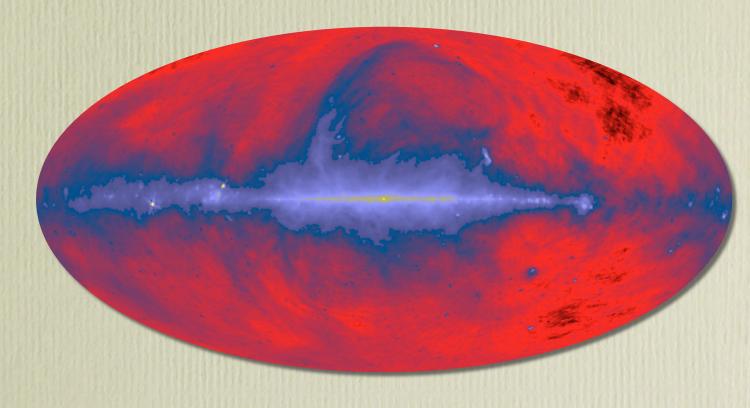
Building an EOR machine: the MWA–LFD

Now that we have a basic idea of the signal we're going after, I'd like to spend the bulk of this talk focusing on how to build an EOR machine? And I'm going to highlight the MWA–LFD my collaborators and I are building in WA and we've optimized for the EOR power spectrum signal.

The EOR is very faint—~20mK—and in many ways observing the EOR is similar in difficulty to CMB E or B mode polarization experiments.

Challenges 1: Foregrounds

- Faint point sources

- Smooth galactic emission

- Galactic radio recombination lines

- RFI

- Others!
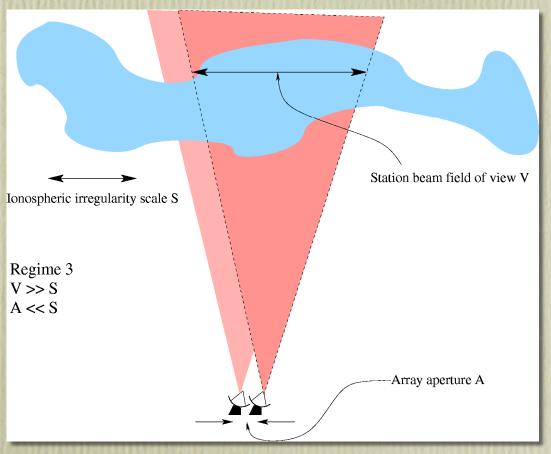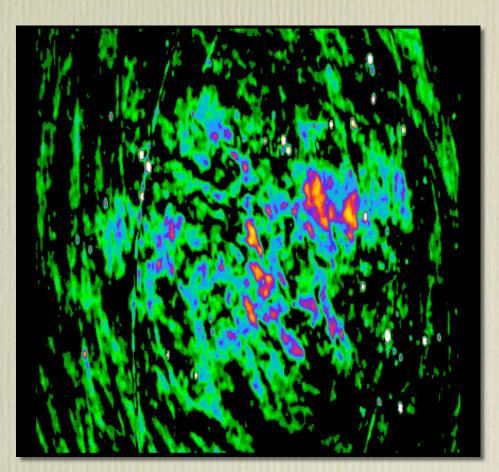
We face a number of challenges... first the foreground are 4-5 orders of magnitude brighter than the signal we are looking for.

Galaxy is a few 100k, dominates our noise budget.

[mention we're observing in the FM an TV bands.]

Challenges 2: Ionosphere & Polarization

Lonsdale (2004)

325 MHz polarized flux, 6° x 6°, 4' beam, 5 K peaks (de Bruyn)

In addition, we have instrumental foregrounds. [Walk through.]

We can work around these challenges in two ways: increasing the sensitivity of the experiment, and carefully controlling the systematic effects.

Step 1: increase sensitivity

TABLE 1.

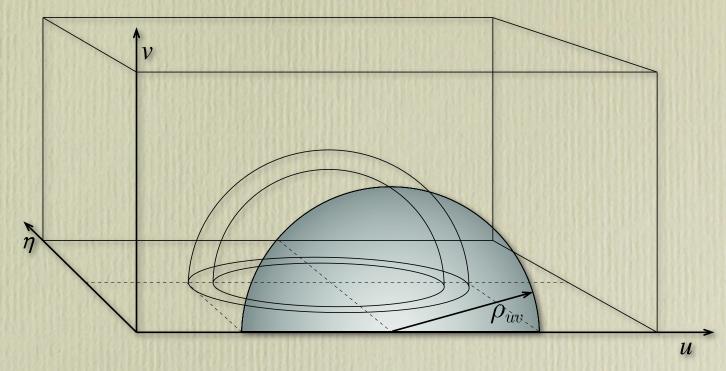|	$A_t\|_{dA}$	$A_t\|_{N_A}$	$dA\|_{A_t}$	B	$\|\mathbf{u}\|$	t
Power Spectrum S/N	A_t^2	$A_t^{3/2}$	$(dA)^{-1/2} \propto$ FOV	$B^{1/2}$	$\|\mathbf{u}\|\,\bar{n}(\|\mathbf{u}\|)$	t

NOTE. — This table lists the scaling relationships of the key equations. In order, the variables in each column are: total array area holding the size of each antenna constant $A_t\|_{dA}$ (adding antennas), total array area holding the number of antennas and distribution constant $A_t\|_{N_A}$ (increasing antenna size), the size of each antenna with the total array area held constant $dA\|_{A_t}$ (dividing area into more small antennas), the total bandwidth B, the sensitivity as a function of wavenumber length $\|\mathbf{u}\|$, and the total observing time t.

Morales (2005)

Survey speed with compact antenna distribution
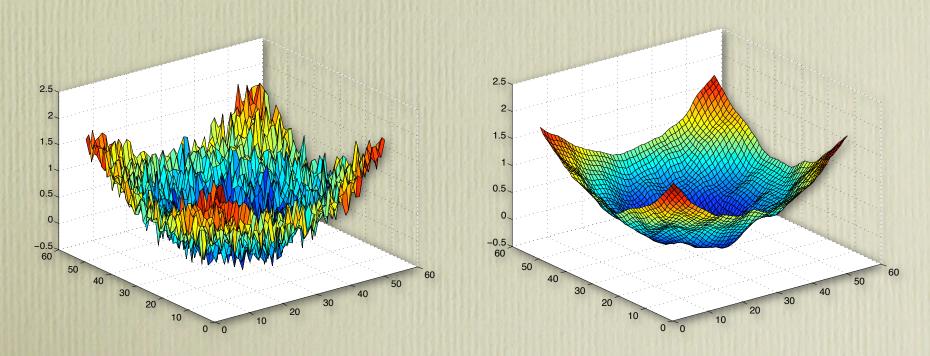
There are several things we can do to address these challenges. In interferometry, each pair of antennas measures one Fourier mode on the sky. For EOR interferometers even very compact antenna spacings can measure small spatial scales in the frequency or line–of–sight direction. So a particular length scale—as shown by the spherical annulus—is measured by all antenna spacing smaller than that scale. Thus we want a very compact antenna distribution.

In addition, the sensitivity is related the the survey speed of the telescope: the volume observed times the collecting area.

Step 2: systematics

What we know about fitting algorithms is goodness-of-fit surface quality → robustness

- Excellent instantaneous point spread function

- Data-rich observations & computation

The second step is to control the systematics. In particular the instrumental calibration needs to be very precise.

One key to this is the spatial dynamic range. As we increase the instantaneous spatial dynamic range—or PSF quality—and the number of calibrator sources, the smoother the goodness–of–fit surface for our calibration becomes, and the more reliable and accurate our calibration.

This ends up driving whole sections of the MWA design.

Mileura Widefield Array– Low Frequency Demonstrator

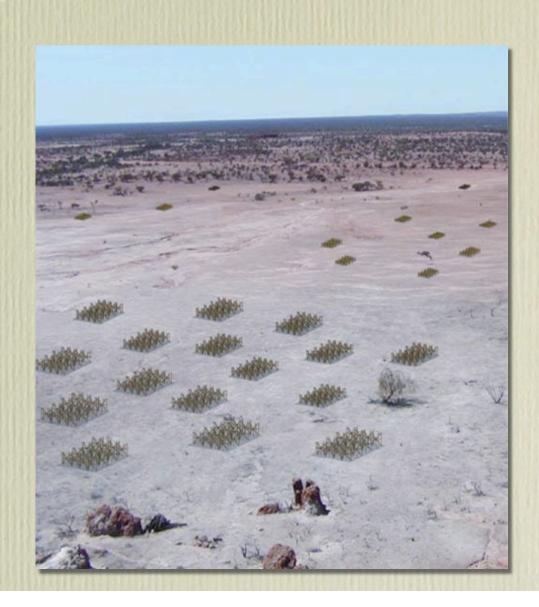So using these design idea, what does the hardware of the MWA–LFD, commonly called the MWA look like?

Here is a picture of one of our prototype antennas in the WA desert.

Mileura Widefield Array – Low Frequency Demonstrator

- 500 16 dipole antennas

- Radio quiet Mileura site

- Full cross-correlation of all 500 antennas

- 80–300 MHz

- Very wide 20°– 40° field of view

- Strict attention to systematics
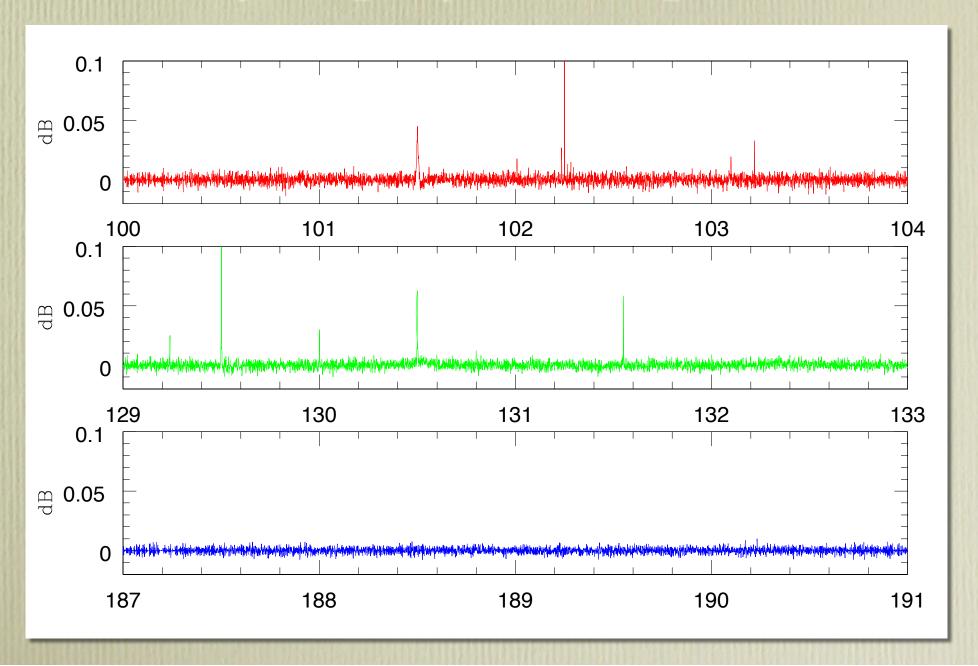
Mileura station

Very radio quiet

The MWA is named after the Mileura Sheep Station, in WA near where it will be located, about here on the map. Mileura Station has a population of 4, 2 adults and 2 children. And this is a picture of the typical scenery. Astronomers are known for going to the ends of the earth for great observing sites, whether it is the summit of Mauna Kea or the Atacama desert of Chile, and Mileura is one of the great radio observatory sites. Because there are so few people, it has never been economical to broadcast FM radio or TV into the outback.
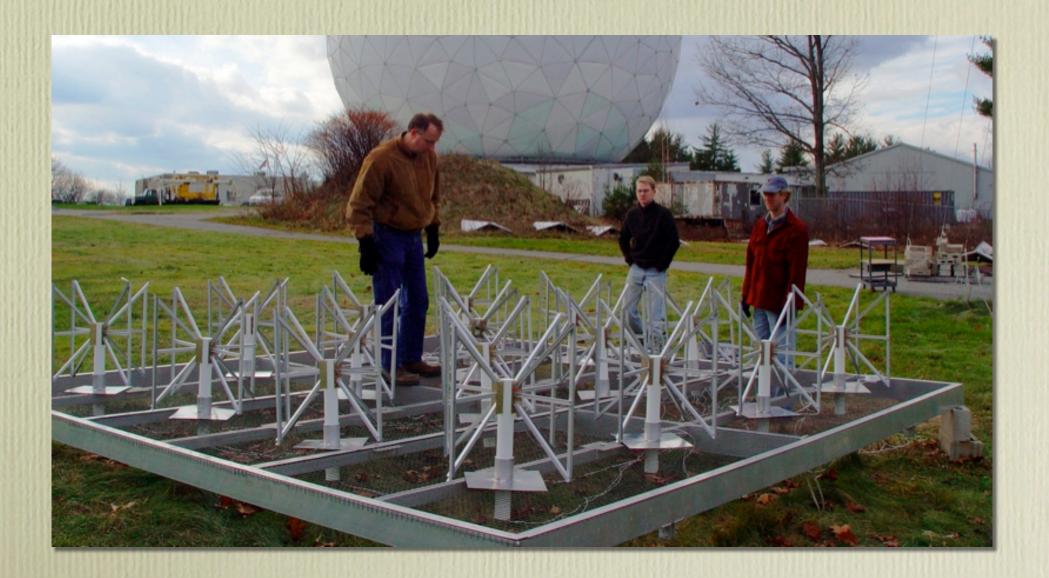
Early deployment spectra

redshifts of 6.5, ~10, and ~13.5 in the FM band.

Compare to FM at the VLA.
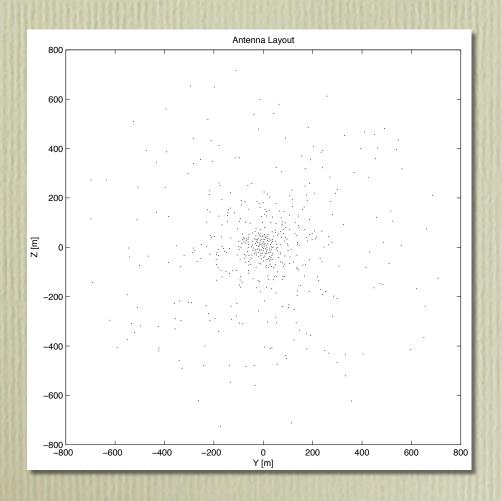
Antenna design
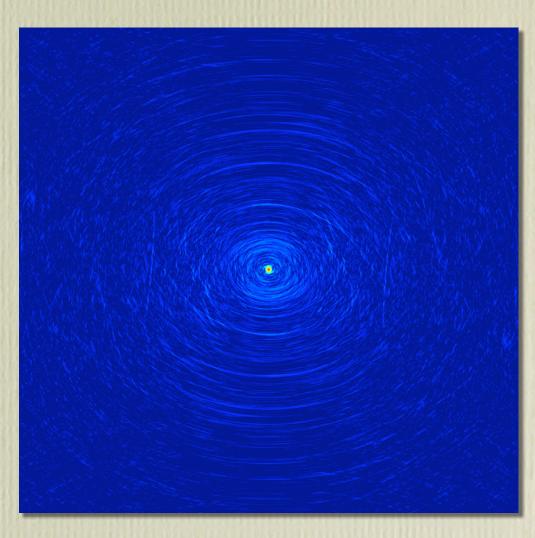
Here is another photograph of the MWA antenna, at the MIT Haystack observatory antenna range.

Made up of 16 dipoles, with delay lines that can be switched in to electronically steer the beam around the sky.

MWA–LFD antenna distribution

[Compact array layout, instantaneous u,v coverage, fabulous integrated PSF]

Goals of MWA-LFD

- Key science drivers:

  - Epoch of Reionization

  - Heliospheric science — FR & IPS

  - Radio transients

This combination of high spatial dynamic range, wide field of view makes it very good at several science drivers:

EOR – both a Stromgren Sphere Experiment being led by Melbourne university, and the larger power spectrum effort which I am leading.

Heliospheric science ....

Radio transients which I am also helping to lead, and has a lot of promise with a 30° FOV. Unfortunately I don't have any time to talk about transients in this talk, but I'd be happy to talk about it during questions or individually.

MWA-LFD Collaboration

MIT Kavli Institute
J. Hewitt, M. Morales, J. Bowman, J. Kasper, M. Tegmark, A. Oliveira-Costa, M. Matejek

MIT Haystack Observatory
C. Lonsdale, R. Cappallo, B. Corey, S. Doeleman, D. Oberoi, J. Salah

Harvard CfA
L. Greenhill, M. Zaldarriaga, D. Mitchell, R. Wayth, L. Hernquist, A. Loeb

U. Melbourne
R. Webster, R. Sault, S. Wyithe

ANU/Stromlo
F. Briggs, J. Kocz

Curtin U.
M. Lynch, D. Herne, B. Stansby
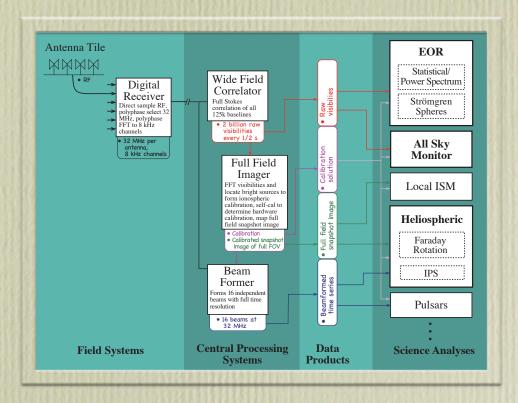
CSIRO/ATNF
J. Bunton, C. Jackson, M. Storey

ALSO
S. Furlanetto, L. Staveley-Smith, B. Gaensler, P. Quinn, Raman Reasearch Institute, ...

The MWA is a US-Australian collaboration of...

Software driven design

We've talked a little about the hardware piece of the array. But the MWA is a digital telescope, and so we need to talk about the digital systems and how we can calibrate the instrument to the necessary precision to understand the whole system.

Software as part of the hardware

- MWA–LFD is designed as a *system* to measure the EOR

- Changes made to the hardware design to make the software processing easier

- Realtime software is an integral part of the system

The MWA was designed as a system...

One of the challenges is that the data rate increases with the instantaneous spatial dynamic range. Because of the large number of baselines for good PSF, we have an enormous data rate: 16 GB/s. This means we cannot save all the data, must calibrate and reduce the data rate in realtime using a ~1 Tflop supercomputer. This choice was made because it can give us higher precision measurements, but the realtime software is an integral part of the the machine.
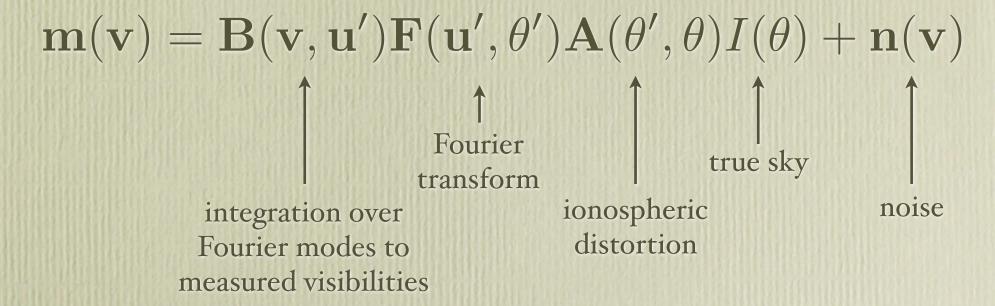
Core realtime software team

M. Morales, R. Sault, D. Mitchell,
S. Doeleman, J. Kasper, R. Wayth

The hardware piece of the MWA that I am currently leading is the RTS.

Laying down the math

Observation:

$$\mathbf{m}(\mathbf{v}) = \mathbf{B}(\mathbf{v}, \mathbf{u}')\mathbf{F}(\mathbf{u}', \theta')\mathbf{A}(\theta', \theta)I(\theta) + \mathbf{n}(\mathbf{v})$$

integration over
Fourier modes to
measured visibilities

Fourier
transform

ionospheric
distortion

true sky

noise

(Tegmark, Zaldarriaga, Morales)

To present the ideas of the realtime processing system, I need to spend a couple of slides laying down the math.

Let's first start with a description of what the instrument does.

Data analysis

Observation:

$$\mathbf{m}(\mathbf{v}) = \mathbf{B}(\mathbf{v}, \mathbf{u}')\mathbf{F}(\mathbf{u}', \theta')\mathbf{A}(\theta', \theta)I(\theta) + \mathbf{n}(\mathbf{v})$$

Data reduction, v1:

$$\hat{I}(\theta) = \left[\mathbf{O}^T\mathbf{N}^{-1}\mathbf{O}\right]^{-1} \underbrace{\mathbf{A}^T(\theta, \theta')\mathbf{F}^T(\theta', \mathbf{u}')\mathbf{B}^T(\mathbf{u}', \mathbf{v})}_{\mathbf{O}^T}\mathbf{N}^{-1}\mathbf{m}(\mathbf{v})$$

inversion/deconvolution

integration point

measurement

noise covariance matrix

The question becomes how to go from the raw visibility measurements back to a good estimate of the sky, and for this we will use the minimally biased estimator framework developed for the CMB. This analysis is based on the fact that it is easy to take the transpose of a matrix operator, but very hard and often impossible to take the inverse.

One way to process this data... [Walk through, stress how the deconvolution does not grow, provides an integration point. For us we must correct both the instrument and the ionosphere before we can integrate.

Central section is moving to a set of coordinates where we can integrate. Is not the only option for coordinate systems.]

Ionospheric correction

$$\mathbf{A}(\theta', \theta) = \delta^D[\theta' - \theta - \delta\theta(\theta, t)]$$

$$\mathbf{A}(\mathbf{u}', \mathbf{u}) = \int d^2\theta e^{i(\mathbf{u}-\mathbf{u}')\cdot\theta + i\mathbf{u}\cdot\delta\theta(\theta,t)}$$

$$\mathbf{A}(\mathbf{u}', \mathbf{u}) \approx \int d^2\theta' e^{i(\mathbf{u}-\mathbf{u}')\cdot\theta'} \left(1 + i\mathbf{u} \cdot \delta\theta(\theta', t) + \cdots\right)$$

$$\approx (2\pi)^2 \delta^D[\mathbf{u} - \mathbf{u}'] + i\mathbf{u} \cdot \int d^2\theta e^{i(\mathbf{u}-\mathbf{u}')\cdot\theta} \delta\theta(\theta, t)$$

$$\delta\theta = \sum_m -ia_m \mathbf{b}_m e^{-i\mathbf{b}_m \cdot \theta}$$
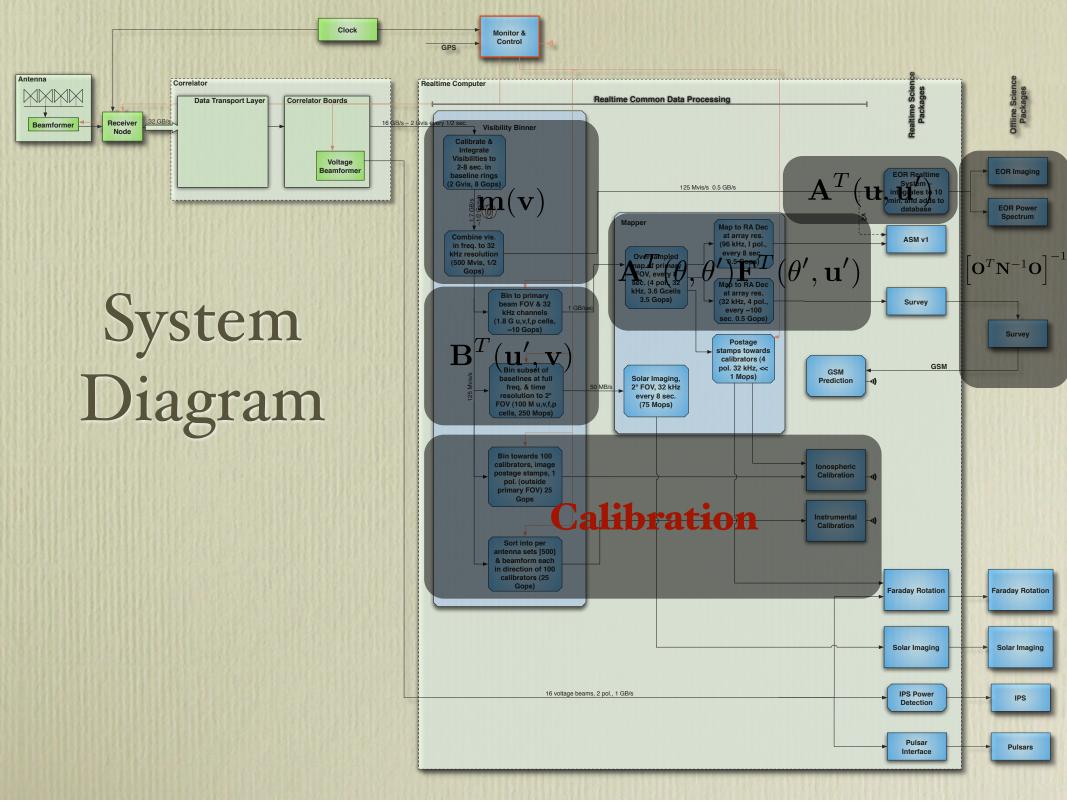
$$A(\mathbf{u}', \mathbf{u}) = \delta^D[\mathbf{u} - \mathbf{u}'] + \sum_m a_m(\mathbf{u}' \cdot \mathbf{b}_m)\delta^D[\mathbf{u} - \mathbf{u}' - \mathbf{b}_m] + \text{cross terms}$$

(Zaldarriaga & Morales; Morales et al.)

Data reduction, v2:

$$\hat{I}(\theta) = \left[\mathbf{O}^T \mathbf{N}^{-1} \mathbf{O}\right]^{-1} \underbrace{\mathbf{A}^T(\mathbf{u}, \mathbf{u}')\mathbf{B}^T(\mathbf{u}', \mathbf{v})}_{\mathbf{O}^T} \mathbf{N}^{-1}\mathbf{m}(\mathbf{v})$$

It turns out that you can correct the ionospheric distortions in the Fourier domain.

[Walk through, end with alternate equation, calculationally more efficient with lower residual errors for the EOR science.]

System Diagram

Clock

GPS

Monitor & Control

Antenna

Beamformer

Receiver Node

32 GB/s

Correlator

Data Transport Layer

Correlator Boards

16 GB/s – 2 Gvis every 1/2 sec.

Voltage Beamformer

Realtime Computer

Realtime Common Data Processing

Visibility Binner

Calibrate & Integrate Visibilities to 2-8 sec. in baseline rings (2 Gvis, 8 Gops)

$\mathbf{m}(\mathbf{v})$

1.7 GB/s ~1/2 Gvis

Combine vis. in freq. to 32 kHz resolution (500 Mvis, 1/2 Gops)

125 Mvis/s 0.5 GB/s

Bin to primary beam FOV & 32 kHz channels (1.8 G u,v,f,p cells, ~10 Gops)

$\mathbf{B}^T(\mathbf{u}', \mathbf{v})$

125 Mvis/s

1 GB/sec

Bin subset of baselines at full freq. & time resolution to 2° FOV (100 M u,v,f,p cells, 250 Mops)

50 MB/s

Mapper

Oversampled map of primary FOV, every 1 sec. (4 pol, 32 kHz, 3.6 Gcells 3.5 Gops)

$\mathbf{A}^T(\theta', \theta') \mathbf{F}^T(\theta', \mathbf{u}')$

Map to RA Dec at array res. (96 kHz, I pol., every 8 sec. 0.5 Gops)

Map to RA Dec at array res. (32 kHz, 4 pol., every ~100 sec. 0.5 Gops)

Postage stamps towards calibrators (4 pol. 32 kHz, << 1 Mops)

Solar Imaging, 2° FOV, 32 kHz every 8 sec. (75 Mops)

Calibration

Bin towards 100 calibrators, image postage stamps, 1 pol. (outside primary FOV) 25 Gops

Sort into per antenna sets [500] & beamform each in direction of 100 calibrators (25 Gops)

16 voltage beams, 2 pol., 1 GB/s

Ionospheric Calibration

Instrumental Calibration

Faraday Rotation

Solar Imaging

IPS Power Detection

Pulsar Interface

Realtime Science Packages

EOR Realtime System - integrates to 10 min. and adds to database

$\mathbf{A}^T(\mathbf{u}, \mathbf{u})$

ASM v1

Survey

GSM Prediction

GSM

Offline Science Packages

EOR Imaging

EOR Power Spectrum

$[\mathbf{o}^T \mathbf{N}^{-1} \mathbf{o}]^{-1}$

Survey

Survey

Faraday Rotation

Solar Imaging

IPS

Pulsars

Let's go back and see how this fits in with the rest of the system. [Quickly point out sections, boxes not to scale with difficulty.]
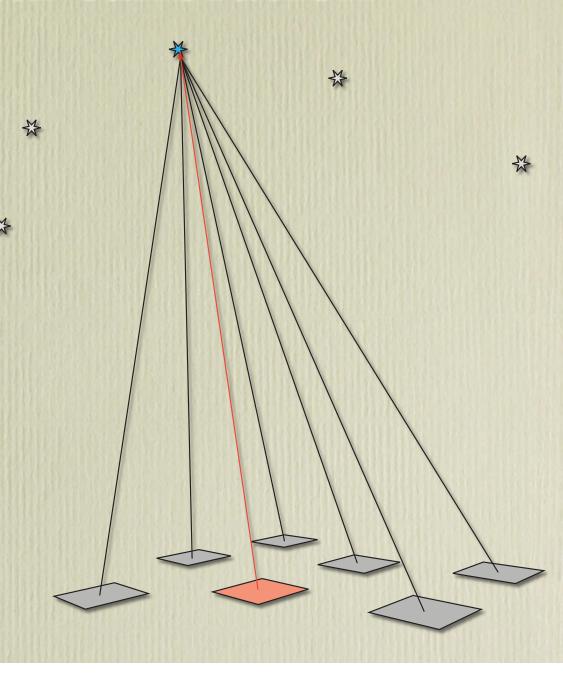
(Walk through, using the mathematical framework.)

(Talk about calibration.) One of the things we have been very careful about is to preserve information deep into the RTS. We have all the visibilities, and our correlator FOV spans horizon to horizon (nothing aliases in). This provides a wealth of information we can draw upon for our calibration algorithms.
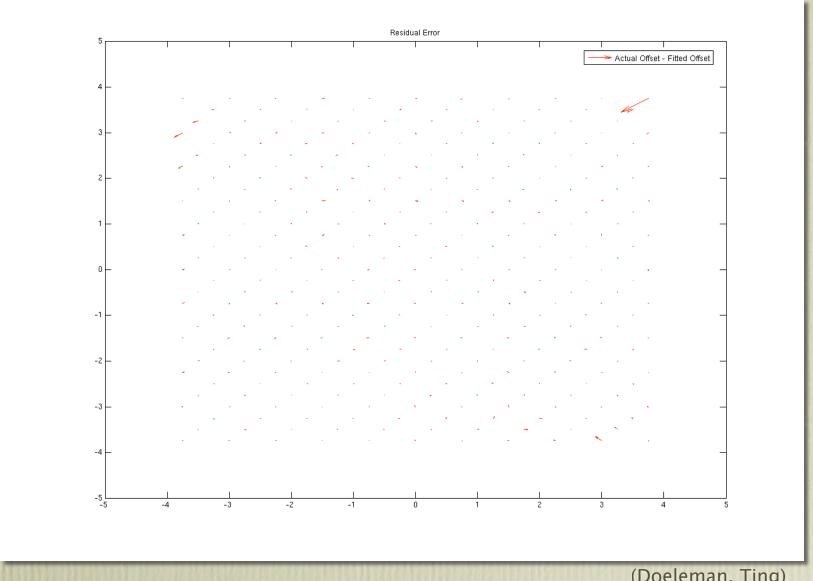
Instrumental calibration

Instrument:

Gain from one
antenna to rest of
array, simultaneously
for all antennas &
100 sources

[Walk though one antenna.

Quickly add simultaneously for 100 sources, all 500 antennas, full polarization. Produces a very rich set of data for constraining the calibration of each antenna.]
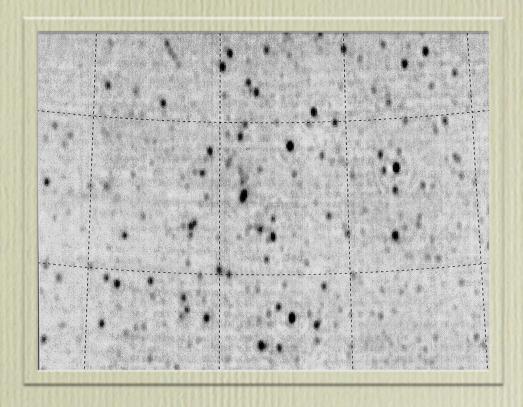
Ionospheric calibration

Residual Error

Actual Offset - Fitted Offset

(Doeleman, Ting)

Up to 1500 sources with known location,
fit every 8 seconds ➤ rubber sheet

RMS errors of approximately 1'' — lots more needs to be learned about the ionosphere

EOR foreground subtraction

Now we've described how we create a precision measurement of the sky. However, we must still subtract off the foreground sources to a precision of ~10e−5.

EOR collaboration

J. Hewitt, M. Morales, R. Webster,
F. Briggs, S. Furlanetto, L. Greenhill, L. Hernquist,
A. Loeb, C. Lonsdale, A. de Oliveira-Costa,
M. Tegmark, S. Wyithe, M. Zaldarriaga

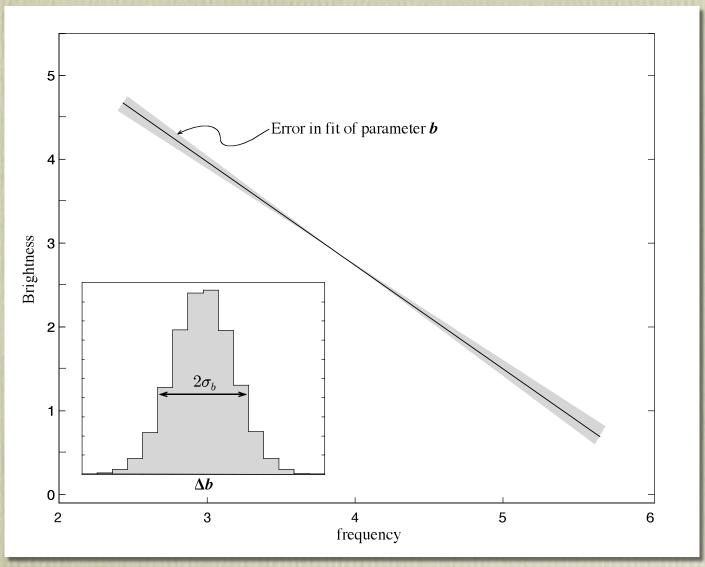The science piece of the MWA that I am leading the EOR Power Spectrum measurement.

Stages of astrophysical foreground subtraction

- Bright source & RFI subtraction

- Spectral fitting

- Parameter estimation, using power spectrum templates

[Multi-stage, removing increasing faint contaminants. But not perfect...]

And a new technique which is unique to the EOR, where we can subtract the average errors introduced in the previous 2 steps.

Spectral fitting

Morales, Bowman & Hewitt (2006)

For example one of the kinds of errors is due to mis–fitting the spectral slopes.

Residual contamination due to this mistake.

Spectral foreground errors

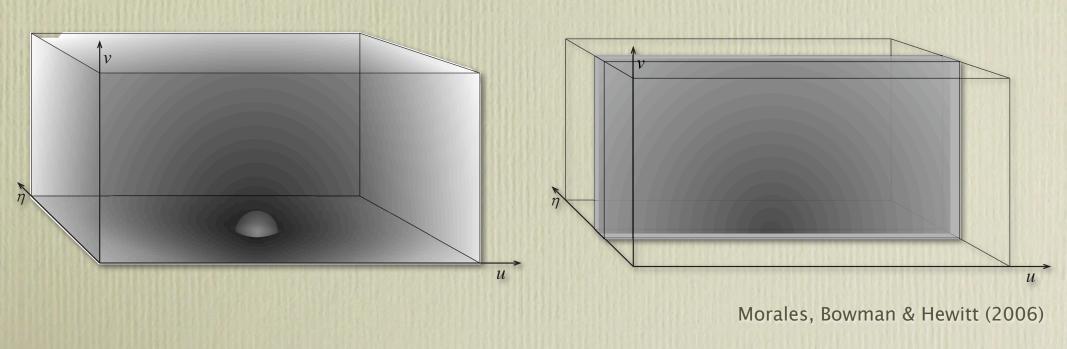$$\Delta S(f) = \Delta a\, df^2 + \Delta b\, df + \Delta c$$

$$\langle P_s(\eta) \rangle = 2\Theta d\Omega B^2 \left[\frac{\sigma_a^2}{\pi^2 \eta^4} + \frac{\sigma_b^2}{\pi^2 \eta^2} + \sigma_{c'}^2 \delta^k(\eta) \right]$$

Mistakes can be written down.

And you can calculate the powers spectrum of these mistakes. Here eta is the line-of-sight wavenumber, and notice that each component has a distinct shape in the three dimensional power spectrum. If you plot this you get something like...

Parameter fitting

- Use templates to separate EOR signal from residual foreground subtraction errors

- Fit both local parameters & their ensemble errors
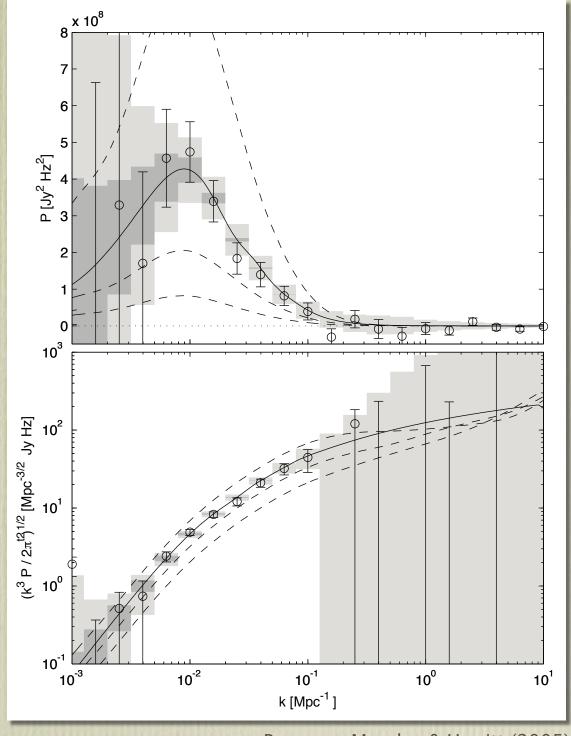

Morales, Bowman & Hewitt (2006)

Notice how this is very different from the 3D shape of the EOR signal.

For each kind of error, whether fitting or model, you can calculate the corresponding power spectrum residual. Final foreground removal step becomes a parameter fit. Allows much better foreground removal.

So now that we have talked about how to measure an extract the faint EOR signal, how sensitive is the MWA?

MWA–LFD power spectrum sensitivity

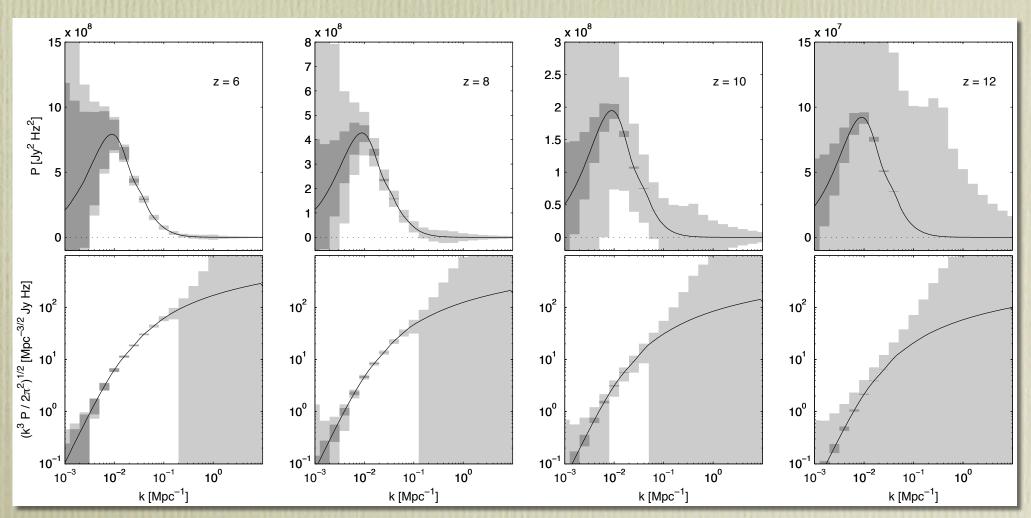z = 8, 360 hours of integration

Bowman, Morales & Hewitt (2005)
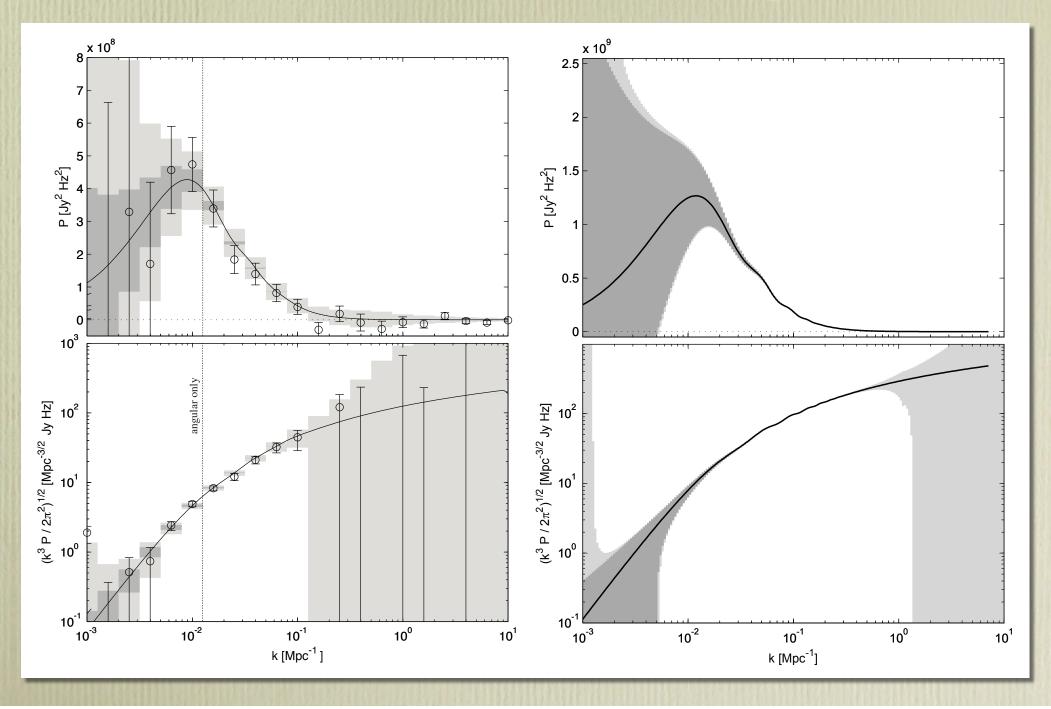
Walk though axes and different error terms.

Look at those error bars! Even though this is a demonstrator class instrument, we have the sensitivity to measure the EOR. The key is controlling the systematics to sufficient precision to extract the signal.

MWA–LFD sensitivity vs. redshift
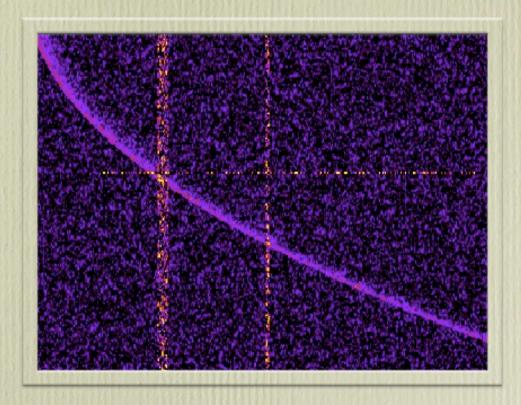

Bowman, Morales & Hewitt (2005)

MWA−LFD vs. MWA5000

MWA-LFD

- ~$10 million instrument, funded

- Data taking starting in late 2008

- Premier EOR instrument

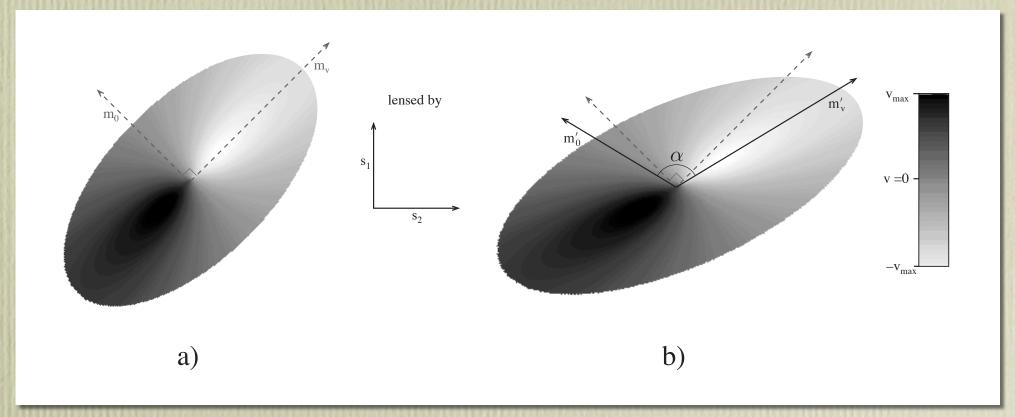 - Strict attention to systematic errors

http://web.haystack.mit.edu/arrays/MWA/index.html

New radio cosmology signatures

The EOR is the primary focus of my research, but over the last few years I have also developed three other new radio cosmology signatures. I'd like to talk about one of them I've been having some fun with recently.

Weak lensing with velocity maps

Morales (2006)

$$\alpha = 2\arctan\left[\frac{(1-\kappa)+\gamma}{(1-\kappa)-\gamma}\right]$$

Weak lensing has become one of the most powerful techniques for measuring spatial distortions and dark energy.
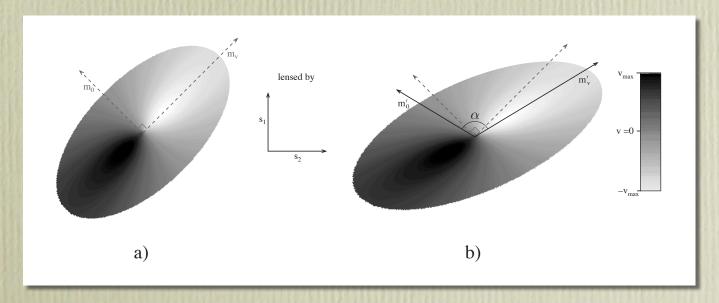
Foreground masses squeeze the images of background galaxies, increasing their ellipticity and slightly aligning the images. However, because the inherent ellipticity of any individual galaxy is unknown, it requires observing very high density of background galaxies, so one can marginalize over the unknown inherent ellipticities. This effect is called ellipticity noise, and is the main driver behind proposed continuum weak lensing surveys at optical and radio frequencies.

This summer I published a paper showing how to work around the ellipticity noise with velocity resolved maps. The basic idea is quite simple and is best shown with a picture...

(End with entire velocity profile... thus more sensitive).

Sensitivity features:

- Reduced number counts, but no ellipticity noise

- Uncertainty in shear is $\propto$ to brightness of the galaxy

- Systematics are different: PSF less important, insensitive to bright knots & intrinsic alignment, sensitive to warped disks, etc.

What are the sensitivity features of this new way of measuring weak lensing? (Do points 1 & 2).

As highlighted by the DETF, systematic effects are often key, effects such as the sagging of an optical telescope on the PSF can bias the results. Very different systematic features.

Prospects

- For HI observations with SKA, neglecting systematics, velocity maps are at least as sensitive as continuum observations

- Continuum and velocity WL can be measured simultaneously with modern correlators

- Systematics will be the key

Morales (2006), ApJL, astro-ph/0608494

So how sensitive is this?

The easiest place to observe this is at radio frequencies, using the HI line.

Again, whether this is at all useful will depend on all the systematic effects, and I have a small proposal before the NSF to explore these effects and perform the first velocity resolved lensing observations at radio frequencies to see if this could be a promising signature.

Conclusion

- Entering a new golden age of radio astronomy

- New EOR observations will allow us for the first time to see the emergence of the first objects

- Help answer how structure formed